Mineralogical Magazine, December 1999, Vol. 63(6), pp. 801–812

Early Palaeolithic bone diagenesis in the Arago cave at Tautavel, France

L. QUATTROPANI[1,*], L. CHARLET[2], H. DE LUMLEY[3] AND M. MENU[1]

[1] Laboratoire de Recherche des Musées de France, CNRS-UMR 171, 6 rue des Pyramides, F-75041 Paris Cedex 01, France

[2] Groupe de Géochimie de l'Environnement, L.G.I.T., CNRS-UMR C5559, Université de Grenoble I (UJF), B.P. 53, F-38041 Grenoble Cedex 9, France

[3] Muséum National d'Histoire Naturelle, Institut de Paléontologie Humaine, 1 rue René Panhard, F-75013 Paris, France

ABSTRACT

Bones from level G in the Arago cave (Tautavel, Southern France, 450 ky) were analysed using a combination of particle induced X-ray and gamma-ray emission (PIXE and PIGME) and X-ray diffraction (XRD). Human occupation and guano production by bats introduced a large amount of phosphate into the cave and as a result a decarbonated pocket was formed in the sediment, characterized by the dissolution of clay minerals, calcite and bones, and by the precipitation of phosphate secondary minerals. The Al released by clay minerals was reprecipitated as crandallite in the few remaining bones, and as montgomeryite with traces of crandallite in the surrounding sediments. Bones within the pocket have very high levels of Al, Fe, F and Zn and often have 'diffusive' type U-shaped concentration profiles. These profiles show that post-mortem uptake of trace elements occurred, and thus that trace element composition has to be used with care in palaeonutritional studies but is indicative of local palaeoenvironment. This uptake is complicated by a large increase in hydroxylapatite crystallinity in Palaeolithic bones compared to modern or more recent ones, as a result of the large P influx which occurred in the Arago cave after the sediment deposition.

KEYWORDS: bone diagenesis, Tautavel, PIXE, PIGME, XRD, apatite, crandallite, montgomeryite.

Introduction

WITHIN an archaeological context, bone remains are among the most important witnesses of past human occupation. However, archaeological interpretations, e.g. population occupancy, can be underestimated if bone remains have been dissolved or altered as a consequence of their interaction with the sedimentary environment. Similarly, palaeodiet or palaeoclimate reconstruction based on the chemical composition of the mineral and/or organic part of bones (Price *et al.*, 1985; Bocherens *et al.*, 1994; Runia, 1987; Parker and Toots, 1980) requires that diagenetic processes have not altered the life-time composition of the bone. For example, Sr and Ba trace element contents from bone mineral are used to discriminate between herbivores and carnivores, with Sr and Ba concentrations reducing through the various trophic levels, as well as to distinguish the importance of terrestrial *vs* marine organisms in subsistence (Parker and Toots, 1980; Price *et al.*, 1985; Runia, 1987). Therefore, for archaeologists as well as for climatologists it is essential to understand the various processes leading to bone alteration, which include a variety of phenomena such as dissolution, precipitation and recrystallization, as well as ion uptake by sorption and diffusion. These processes, of course, depend on the physical and chemical characteristics of the burial environment, such as the groundwater and sediment composition, the soil pH, redox potential, temperature regime, porosity or texture. Many studies have therefore been

* Current address: Institut de Physique, Université de Fribourg, Pérolles, CH-1700 Fribourg, Switzerland

© *1999 The Mineralogical Society*

devoted to the evaluation and understanding of diagenesis, to the impact of environment on this diagenesis and to the effects of diagenesis on bone composition and on archaeological records (Parker and Toots, 1980; Badone and Farquhar, 1982; Henderson *et al.*, 1983; Lambert *et al.*, 1985; Kyle, 1986; Williams, 1988; Price *et al.*, 1992; Iacumin *et al.*, 1996). None of these, however, addressed the effect on bone conservation of excretions such as the large post-mortem P influx which characterizes the Palaeolithic sediment found in the Arago cave.

The Arago cave (Caune de l'Arago) at Tautavel is one of the most important Palaeolithic sites in Europe. The skull of the Tautavel Human (Lumley and Lumley, 1971), dated 450 ky, was found at this site and is one of the oldest human remains in Europe. As the result of a long human occupation in the cave and, subsequently, guano production by bats, large amounts of phosphate have been introduced. Partial dissolution of this phosphate and its subsequent redeposition in sediment and in bones as Ca- and Ca-Al phosphates have produced a geochemical sequence of extreme diagenetic alteration of buried bones which will be discussed in this paper.

Ion beam analyses, such as particle induced X-ray and gamma-ray emission (PIXE and PIGME) were used to determine quantitatively the sample post-mortem contamination, even at trace level, and to examine the elemental distributions across bone transverse sections. These techniques, which have been used in the past to analyse archaeological bones excavated from a range of different burial environments (Coote and Vickridge, 1988; Boscher-Barré *et al.*, 1992; Elliott and Grime, 1993) are applied here to study the effect of a large external influx of P and consequent apatite recrystallization, on the post-mortem evolution of bones. They are combined with XRD to provide a structural characterization of the bone material and give information about dissolution and recrystallization processes.

Study site

The Arago cave is located in an important karstic system. It is now a large cavity, >35 m long and ~7–10 m wide, situated 80 m above the present bed of the Verdouble, a river flowing at the bottom of the Tautavel plain, located in southern France at the base of the southern slope of Corbières Mountains, 19 km northwest of Perpignan. In the cave, there are sediments >15 m thick, deposited during several Pleistocene climatic periods between 690 and 92 ky, both by wind and by percolating waters. This sediment has been the topic of numerous studies which are summarized hereafter (Beiner, 1983; Lumley *et al.*, 1984; Mosser *et al.*, 1992; Perrenoud, in press). The sand fraction is composed of quartz, schist and mica. The clay fraction (<2 μm) is made of calcite and various phyllosilicates (well crystallized kaolinite, illite and a swelling smectite). During periods of sedimentation, the cave was, however, also used by prehistoric people. The settlements are revealed by the presence of layers of herbivore bones, stones, pebbles, products of the lithic industry (quartz, flints, etc.) and human remains (Fig. 1).

The top sediment layer consists of thick continuous stalagmitic calcite layers, dated between 400 and 92 ky, interbedded with archaeological sediments. Fissures appeared in the ceiling of the cave from 400 ky, followed in the last 35 ky by the opening of a hole extending up to the plateau on top of the cave. Below this hole the stalagmitic layer of calcite is absent and has probably been dissolved by infiltrating water. Here, the deposits comprise a decarbonated pocket, rich in phosphates, which is characterized by an almost complete dissolution of archaeological remains such as bones or calcareous stones. The few remaining bones have been studied in detail and are discussed below. Limestone fragments are extremely rare. The sand fraction and lithic industry remains are similar to those found in the surrounding sediment (Fig. 1); however, the <2 μm fraction has been deeply altered. The overall result of this alteration is a decrease in sediment bulk density (from 1.3 g cm^{-3} outside the pocket to 0.9 ± 0.3 g cm^{-3} within), $CaCO_3$ content (from 25.3 ± 1.5 to 3.4 ± 1 wt.%) and pH (from 9.1 ± 0.3 to 8.6 ± 0.2). Calcite has to a large extent been replaced by hydroxylapatite, $Ca_5(PO_4)_3OH$ (almost devoid of carbonate) which is finely disseminated throughout much of the sediments, and is commonly a cement. This apatite ('apatite I') is white to pink in colour, mostly amorphous, and is present mainly at the bottom of the pocket. Carbonate-hydroxylapatite (dahllite) occurs as rings surrounding limestone blocks. Apatite I is covered by sand-size radial crystals of montgomeryite ($Ca_4MgAl_4(PO_4)_6(OH)_4.12H_2O$), the abundance of which decreases toward the top and the centre

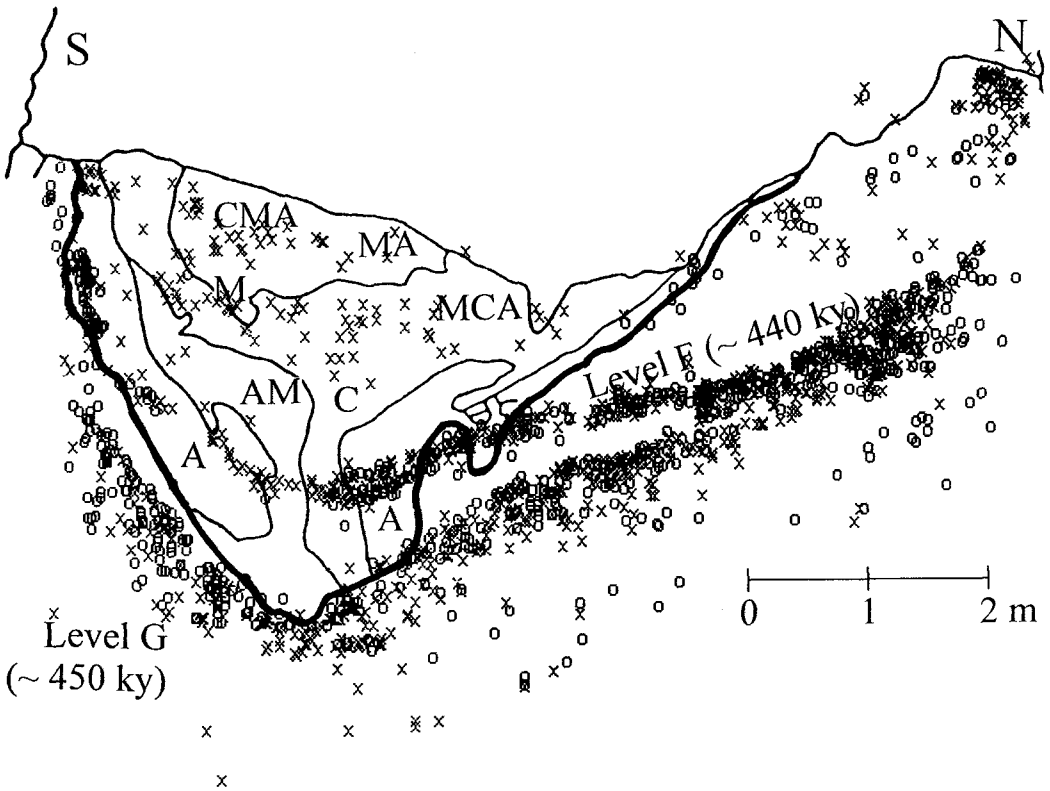

FIG. 1. Cross-section of the Arago cave soil, with the distribution of the archaeological materials and the phosphate minerals within the decarbonated pocket. The bold line indicates the boundary of the decarbonated pocket, the circles indicate buried bones and the crosses, the lithic industry remains. Within the decarbonated pocket, A indicates the presence of apatite, C, that of crandallite, and M, of montgomeryite (Beiner, 1983; Pois, 1997).

of the pocket. In some places, 5 μm microcrystalline crandallite ($CaAl_3(PO_4)_2(OH)_5.H_2O$) covers all particles, including montgomeryite. Montgomeryite, and to a lesser extent crandallite, appear in the sediment where clay minerals, and in particular smectite, disappear. Some poorly crystallized kaolinite is present, together with interstratified illite-vermiculite. Clay minerals are furthermore de-ferritized and are extremely poor in Mn. A second type of apatite ('apatite II') covers the secondary minerals mentioned above with a 10–15 μm thin coating. This apatite II is either amorphous or present as small crystalline needles. It is thought to be a secondary mineral because original apatite crystals in bones are only $20 \times 5 \times 5$ nm in size (Simkiss and Wilbur, 1989). Its abundance and crystallinity increase towards the top of the pocket (Fig. 1). Finally, throughout the entire pocket, the pores have a subsequent filling of Mg calcite (Perrenoud, in press).

Nowadays the 'decarbonated pocket' is characterized by a very low porosity and is surrounded by a porous calcareous siliceous sediment which acts as a capillary barrier. The pocket therefore remains nearly saturated with water, whereas the surrounding sediment is often dry. Manganese (and to a lesser extent Fe) is depleted in the pocket, but accumulates as Fe, Al, Mg and Zn rich manganous oxide concretions at the edges of the pocket.

Materials and methods

Materials

Ten bone fragments (T1 to T10, Table 2) were selected from level G, i.e. from the upper part of the Arago cave archaeological sequence. This is the level in which the skull of the Tautavel Human was found and dated at 450 ky. The samples used in the present study are fragments of

TABLE 1. Concentrations of elements corresponding to the measurements presented in Fig. 2. The Na to Ca concentrations were obtained from the PIXE spectra measured with the low energy X-ray detector (spectra in Fig. 2), Mn to Sr concentrations were obtained from the PIXE spectra measured simultaneously with the high energy X-ray detector and the F concentration was measured by PIGME, using the $^{19}F(p, p'\gamma)^{19}F$ nuclear reaction emitting a γ-ray of 197 keV. All values, unless otherwise stated, are given as ppm ($\mu g/g$). Concentrations below the limit of detection are denoted n.d. (not detected). The error values are the statistical errors on the measurements, given by the GUPIX software, except in the case of F, where they are the statistical errors on detector counts evaluated as the square root of the count area

	Inside the decarbonated pocket (Level G)	Outside	Modern bone
	T1	T3	MB1
F	2670 ± 110	310 ± 40	150 ± 20
Na	2200 ± 440	3300 ± 500	9070 ± 450
Mg	1950 ± 250	1250 ± 250	7270 ± 260
Al	19500 ± 300	n.d.	n.d.
Si	4660 ± 350	n.d.	n.d.
P	16.74 ± 0.07%	17.15 ± 0.07%	17.91 ± 0.05%
S	950 ± 180	600 ± 200	1670 ± 180
Cl	670 ± 100	n.d.	700 ± 90
Ca	38.13 ± 0.07%	40.58 ± 0.08	38.35 ± 0.08%
Mn	340 ± 15	n.d.	n.d.
Fe	3430 ± 30	15 ± 8	n.d.
Cu	30 ± 5	30 ± 6	n.d.
Zn	1160 ± 15	210 ± 10	120 ± 5
Sr	820 ± 25	340 ± 20	190 ± 10
Ca/P	2.28	2.37	2.14

long bones from large herbivores, such as horses or wild sheep. The bones were identified and classified according to colour and density (Moigne, pers. comm.). They were then prepared as transverse sections. A few of the more fragile bones were first embedded in a polyester resin, in order to reinforce their brittle structure, before being cut with a diamond saw. The other samples were cut without resin pre-treatment. The resin embedding was shown not to influence the measurements of the elemental concentrations. Section surfaces were then polished with silicon carbide paper (5 μm grain size), rinsed in deionized water and dried at room temperature (or in an oven at 80°C) for at least 12 h. A sample of a modern unaltered sheep bone was prepared in the same way, as a control (MB1).

For bone X-ray powder diffraction analyses, diamond saw cuts were finely ground manually in an agate mortar. Bone apatite crystallinity was also characterized on modern bone and fossil bones from two sites, with strikingly different environments: a calcareous Upper Palaeolithic rock shelter (Les Peyrugues, Lot, France, 13 to 26 ky) and a sandy, very salty, environment in the La Chrétienne M massaliot shipwreck (Var, Mediterranean Coast, France, ~500 BC).

PIXE and PIGME measurements on archaeological bones

The elemental composition of the mineral part of bones was determined using particle induced X-ray emission (PIXE) analysis on AGLAE (Accélérateur Grand Louvre d'Analyse Elémentaire), the particle accelerator facility at the LRMF, Paris, France (Menu *et al.*, 1990). This is a very sensitive and non-destructive technique which provides the major, minor and trace elemental composition of the sample surface, with a depth of analysis of some tens of micrometers, for all elements heavier than Na (i.e. with atomic number $Z>10$). The limit of detection is commonly between 5 and 30 ppm for the heavy trace elements (heavier than Ti) and between 100 and 300 ppm for the light elements. AGLAE is an electrostatic tandem 2 MV

accelerator (6SDH-2 2 MV tandem Pelletron from National Electrostatics Corporation) entirely devoted to the analysis of archaeological and art objects. For this study, we used the external beam facility in a configuration described previously by Calligaro *et al.* (1996). The proton beam hits the sample surface at an energy of 2.8 MeV, after going through a Kapton foil and a He atmosphere. Emitted X-rays are detected using two Si(Li) detectors, forming a 45° angle with the incident beam. The first detector is used to detect the low energy X-rays emitted by the light elements, i.e. mainly P and Ca in the case of bone. The second detector, equipped with a 49 μm Al filter to attenuate X-rays emitted by the bone matrix elements, is used to detect elements heavier than Fe. The PIXE spectra are processed using the GUPIX package (Guelph PIXE software package (Maxwell *et al.*, 1988)). Oxygen is estimated so that the sum of oxides equals 100%, for the low energy X-ray spectra. The Fe content of bone samples is usually too low for it to be used as an internal standard, so the high energy X-ray spectra are processed by fixing the value of the solid angle. This value is determined by the GUPIX processing of glass standards (Brill A, B and D from Corning) in the same geometrical conditions, using Fe as an internal standard. Measurements on these glass standards give elemental compositions in very good agreement with the certified values and confirm the validity of PIXE in obtaining quantitative compositional data.

In order to determine the F content of the bones, the technique of particle induced gamma-ray emission (PIGME) was used simultaneously with the PIXE. The F content was measured by means of two $^{19}F(p, p'\gamma)^{19}F$ prompt nuclear reactions emitting γ-rays of 110 and 197 keV, respectively. As a F standard, we used a polished crystal of fluorapatite; the amount of F in this standard was determined in solution by potentiometry using a F specific electrode as 3.27 wt.%.

The bone sections were placed directly in front of the external proton beam for the PIXE and PIGME analyses. It was not necessary to coat the samples with a conductive layer as the charge was dissipated in air. The beam diameter is ~0.7 mm. By moving the sample in front of the beam between each measurement and precisely recording the length of the step (~1–2 mm), concentration profiles along the bone sections are determined. The beam diameter limits the spatial resolution and the measured profiles are therefore a convolution of the real bone concentration profile and the beam diameter. However, even if these profiles are measured at a macroscopic scale as compared to the microscopic structures in bones (e.g. interstitial lamellae, Haversian canals, pores, hydroxylapatite crystals), they give the general trend of the contamination penetration into the bones. New developments to reduce the external beam diameter are in progress, and they will allow improvement of the spatial resolution of the concentration profiles in future measurements.

X-ray powder diffraction

The crystallinity of apatite, within bones, was determined using X-ray powder diffraction (Siemens D5000 diffractometer). The crystallinity index, CI, a semi-quantitative estimate proposed by Person *et al.* (1995), is defined as $CI = (h(202) + h(300) + h(112))/h(211)$. In this formula, $h(202)$, $h(300)$ and $h(112)$ are the heights of the peaks corresponding to the respective hydroxylapatite X-ray reflections. The peak height is defined as the difference between the average intensity recorded at the top of the peak and the intensity of the 'valley' separating the peak from the previous one or, for $h(211)$, the base line measured between 32° and 43°2θ with Co-$K\alpha$ radiation. The CI values presented in Table 2 are averages of two or three measurements.

Results

Bones within a given archaeological level (level G) but located inside and outside the decarbonated pocket are very different in chemical composition and structure. Figure 2 shows typical PIXE spectra representative of the two environments. They were measured at the centre of the bone cortices, away from the edges and are thus considered to be characteristic of a mean composition of these bones. These spectra are compared to one measured on the modern bone (Fig. 2*c*) under the same conditions. Table 1 gives the numerical values of the elemental composition for these three measurements. The light elements, such as Na or Mg, are present at lower concentrations in the archaeological bones than in the modern bone, regardless of their origin. This indicates a tendency for these elements to be leached out by the groundwater during burial, due to the high mobility and low

TABLE 2. Hydroxylapatite crystallinity index (CI) values of archaeological bones from the Arago cave, Les Peyrugues and La Chrétienne M sites as compared to that of modern bone. The error in the CI values is ~0.02

Site			Bone No.	CI
Arago cave	Level G	inside the decarbonated pocket	T1	0.94
Tautavel		(450 ky)	T2	0.80
	Level G	outside the decarbonated pocket	T3	0.49
		(450 ky)	T4	0.46
			T5	0.36
			T6	0.07
			T7	0.36
			T8	0.61
			T9	0.58
			T10	0.64
	Level H	outside the decarbonated pocket		
		(500 ky)	T11	0.29
	Level L	outside the decarbonated pocket		
		(550 ky)	T12	0.20
Les Peyrugues		(13 to 26 ky)	P1	0.01
Calcareous Upper Palaeolithic rock shelter (Lot, France)			P2	0
			P3	0.14
			P4	0.16
			P5	0.09
			P6	0.09
			P7	0
			P8	0.03
La Chrétienne M		(500 BC)	Ch1	0
Shipwreck (Mediterranean Coast, France); sandy, very salty environment			Ch2	0.01
Modern Bone			MB1	0

sorptive capacity of these ions (Parker and Toots, 1980; Lambert *et al.*, 1985; Boscher-Barré *et al.*, 1992; Price *et al.*, 1992). For the other elements, the chemical composition of bone located outside the pocket (Fig. 2*a* and Table 1) is similar to that of the mineral part of unaltered modern bone (Fig. 2*c*, Table 1), and is characterized by low levels of Al, Si, Mn, Fe, Zn and Sr. By comparison, the bones found in the decarbonated pocket are enriched in F, Al, Fe and Zn, and, to a lesser extent Si, Mn and Sr (Fig. 2*b*, Table 1).

The differences between the two groups of bones are even more obvious when the concentration profiles measured across the bone sections are compared (Figs 3, 4). Bones from within the decarbonated pocket have a high Al content, >1 wt.% throughout the whole bone section, whereas bones from the same level, but buried outside the pocket, contain <0.2 wt.% Al (Fig. 3*a*), with some of them, not represented on Fig. 3*a*, being free of detectable Al throughout the whole profile. Iron (Fig. 3*b*), F (Fig. 4) and Zn (data not shown) generally show similar profiles to Al, but at lower concentrations. All bones, from inside or outside the pocket, have rather constant Ca to P weight ratios, in the range of 2.22 to 2.38. These values are slightly above the ratio found in modern bones (~2.14) and in stoichiometric hydroxylapatite (2.16) (Runia, 1987), and indicate a small enrichment in Ca with respect to P in all bones studied.

X-ray diffraction measurements for all bones show that hydroxylapatite is the major mineral present. In the decarbonated pocket bones contain also a small amount of crandallite (Fig. 5), but no detectable montgomeryite. In the sediment, crandallite is rare and only present as coatings on montgomeryite. The majority of bones from the Arago cave (level G and also other levels) have a high crystallinity index (Fig. 6), compared with modern bones or with bones from more recent archaeological sites which have not been

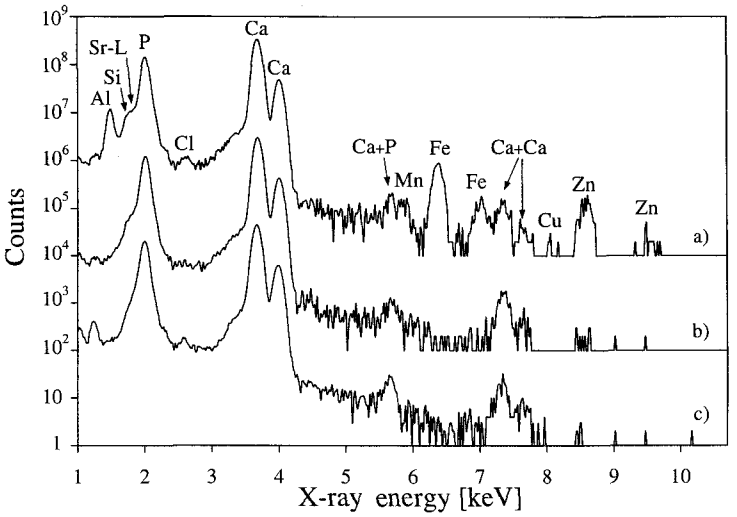

FIG. 2. PIXE spectra obtained with the low energy detector, measured at the centre of bone cortices for two bones representative of the two zones in the Arago cave, located (*a*) inside the decarbonated pocket (bone T1, Tables 1 and 2) and (*b*) outside of it (bone T3, Tables 1 and 2), compared with (*c*) the equivalent PIXE spectrum measured at the centre of the modern bone (bone MB1, Tables 1 and 2). The Si peak is not separated from that of P, because of the presence of the L lines of Sr. The measurement conditions were: incident proton energy on target – 2.8 MeV; beam diameter – ~0.7 mm; integrated charge – ~0.18 μC; acquisition time – ~300 s per spectrum; detector resolution – 150 eV. The Ca+P and Ca+Ca represent the pile-up peaks of Ca and P, and Ca only, respectively. The upper spectra are each shifted on the *y*-axis by two orders of magnitude in order to separate the graphs. Numerical values of the elemental concentrations for these spectra (processed with the GUPIX software) are given in Table 1.

exposed to a phosphate influx, such as those found in Les Peyrugues or in the La Chrétienne M shipwreck. The CI values are greater inside (CI $\geqslant 0.80$, Table 2) than outside the decarbonated pocket (CI $\leqslant 0.64$, Table 2).

Discussion

Bone diagenesis involves a variety of complex and interrelated processes and reflects the interaction of the bone material with its environment. In the case of bones from level G in the Arago cave, all of which show evidence of post-mortem alteration but to varying degrees, we can distinguish two groups.

Bones outside the decarbonated pocket have an elemental composition close to that of the modern bone. They were however exposed to diagenetic processes, as revealed by a typical U-shaped profile for some elements (Badone and Farquhar, 1982; Henderson *et al.*, 1983; Williams, 1988; Millard and Hedges, 1995). Indeed they often show a slight enrichment near the bone surfaces indicating a contamination by diffusion of the elements present in the sedimentary environment. Typical U-shaped profiles were often found for Fe and Al (Figs 3*a*,*b*). Iron is known to be adsorbed or coprecipitated by phosphate minerals. Near the bone surfaces, Fe oxides and clay particles may also fill pores and voids (Kyle, 1986; Pate and Hutton, 1988; Elliott and Grime, 1993). Fluorine presents more irregular profiles with a low mean concentration (corresponding profiles in Fig. 4). Fluorine is known to substitute for hydroxyl ions in hydroxylapatite, eventually leading to fluorapatite formation (Michel *et al.*, 1996). A high crystallinity index measured by XRD indicates the presence of post-mortem alteration processes in the form of recrystallization in the bone apatite.

In the decarbonated pocket, crandallite, an Al phosphate, is present in bones. This indicates that the bones must have been subject to a dissolution recrystallization process (the formation process is discussed in detail below), and is also confirmed by the much higher CI values measured in these

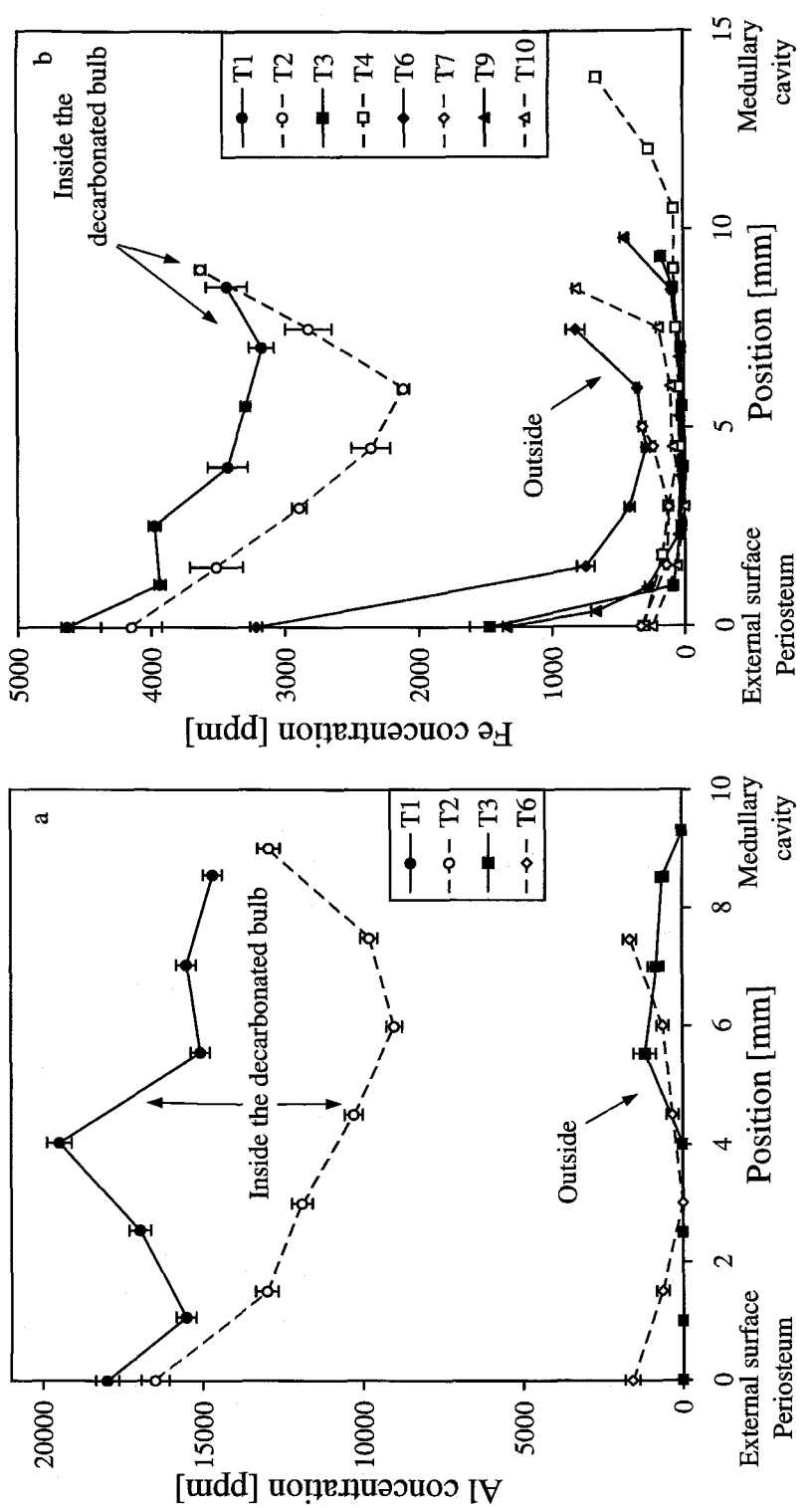

FIG. 3. PIXE concentration profiles for (*a*) Al and (*b*) Fe measured on transverse sections of bones from level G (450 ky). The circles correspond to bones inside the decarbonated pocket (bones T1 and T2, Table 2) and the other symbols to bones located outside the pocket. The error bars represent statistical errors on the measurements, given by the GUPIX software. The beam diameter was ~0.7 mm and the detector resolution, 150 eV (Al) and 180 eV (Fe).

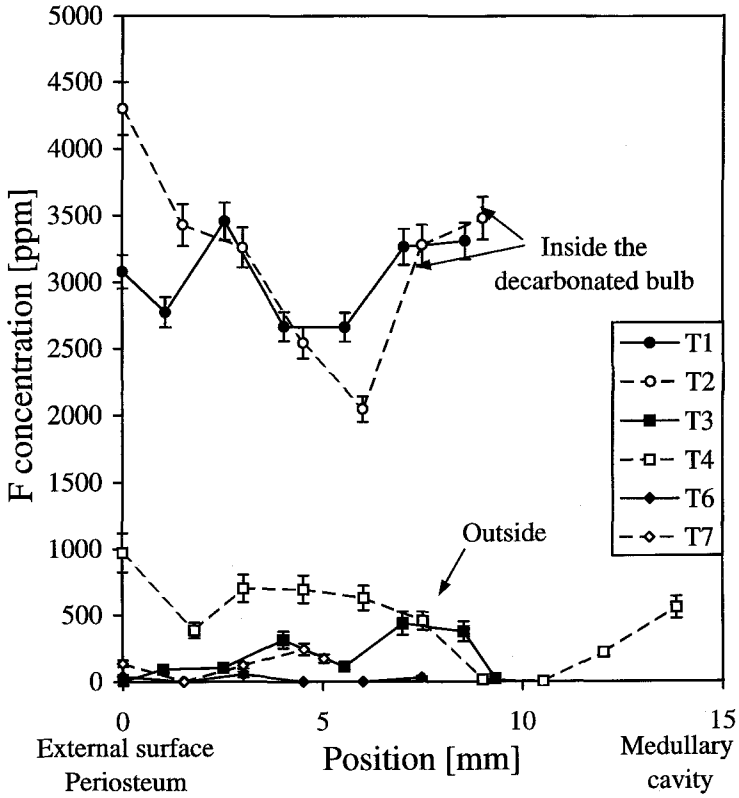

FIG. 4. Fluorine concentration profiles measured by PIGME (using the $^{19}F(p, p'\gamma)^{19}F$ nuclear reaction emitting a γ-ray of 197 keV) on transverse sections of bones coming from level G (450 ky). The circles correspond to bones inside the decarbonated pocket (bones T1 and T2, Table 2) and the other symbols to bones located outside of the pocket. The error bars represent statistical errors on detector counts evaluated as the square root of the count area. The beam diameter was ~0.7 mm and the detector resolution, 1.7 keV.

bones. The Al concentration is mainly the result of the presence of crandallite and the corresponding Al profiles in Fig. 3*a* show that the crandallite is formed throughout the bone, with a clear Al enrichment near the bone surfaces. High concentrations of Fe, F, and to a lesser extent Zn, are strongly correlated with that of Al. The four elements seem therefore to co-precipitate during the formation of crandallite. However, the F content in bones in the decarbonated pocket remains, at ~0.3 wt.%, more than ten times lower than in pure fluorapatite (3.77 wt.%). Finally, there are also elements which are only slightly affected by diagenesis. This is the case for Sr, whose concentration, even for bones within the decarbonated pocket, remains quite close to that found in modern bones. However some U-shaped profiles are also observed, which indicate that this element is incorporated, to some extent, into archaeological bones during diagenesis and thus that care must be taken in dietary interpretations of the bone contents of Sr.

A reconstruction of the Arago cave history might be as follows. The original sediment in the cave was deposited 400 ky ago by wind and water. It is a combination of a calcareous and siliceous sandy sediment, together with layers of Palaeolithic bones (<20% in volume). There is also evidence of human occupancy in terms of lithic industry and artefacts, mainly of quartz, quartzite and marl. Bats would have then settled in the cave, and produced large amounts of guano. This hypothesis is supported by the fact that the amount of P present nowadays in the decarbo-

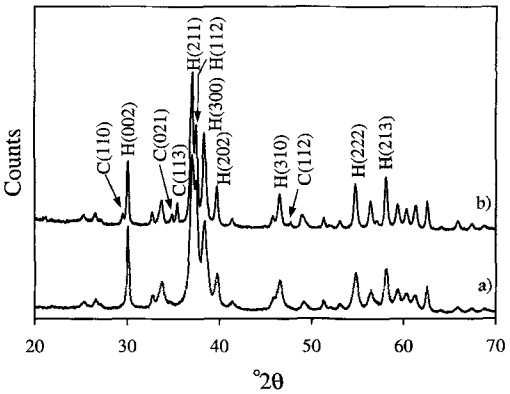

FIG. 5. X-ray diffraction patterns between 20° and 70°2θ, with Co-$K\alpha$ radiation (λ = 1.789 Å), for bone samples (*a*) outside the decarbonated pocket (bone T3, Table 2) and (*b*) inside of it (bone T1, Table 2). Major hydroxylapatite and crandallite reflections are indexed (labelled H and C, respectively). The measurement conditions were: steps of 0.02°; 12 s acquisition time per step, with a sample rotation of 60 revolutions/min; a thin Fe filter is used to absorb the Kβ line of cobalt.

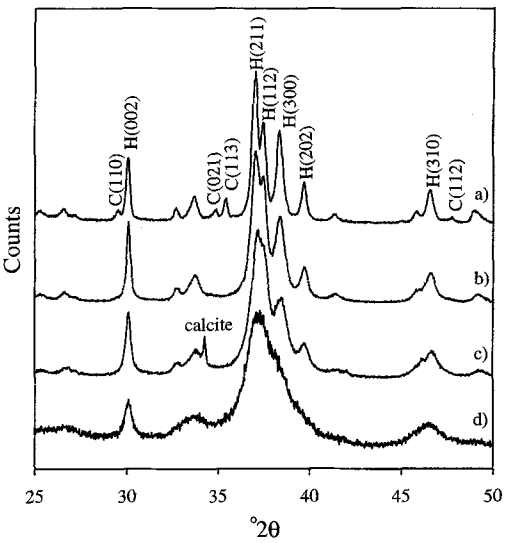

FIG. 6. X-ray diffraction patterns between 25° and 50°2θ, with Co-$K\alpha$ radiation, for bones showing important variations in their crystallinity index. Patterns (a) and (b) are portions of the diagrams shown in Fig. 5 for bones from level G of the Arago cave, inside (bone T1, Table 2) and outside the decarbonated pocket (bone T3, Table 2), respectively. Patterns (c) and (d) are from a bone from the Les Peyrugues site (bone P4, Table 2) and from the modern unaltered bone (bone MB1, Table 2), respectively. The experimental conditions were the same as in Fig. 5, except for the modern bone (pattern d) where the acquisition time is 24 s per step.

nated pocket is orders of magnitude larger than the amount of P present initially as bone in the pocket, estimated on the basis of the relatively homogeneous bone density in the archaeological layers, outside the pocket (Fig. 1). The presence of fissures and ultimately of a hole in the cave ceiling led to the dissolution of the P originally present in guano and its transport in the liquid phase through the stalagmitic sediment upper layer aperture. With this large P influx, an extensive recrystallization process has occurred, leading to bone apatite of high crystallinity (Fig. 6).

Before the influx of P, the clay fraction of the sediment was probably a mixture of calcite, smectite and kaolinite mixed with bone carbonate hydroxylapatite. The paragenesis of a mixture of calcite, montmorillonite and fluor- and carbonate-substituted apatite was studied by Vieillard *et al.* (1979) in a detailed thermodynamic and field study and shown to occur in three steps: (1) disappearance of calcite; (2) dissolution of montmorillonite and precipitation of kaolinite; and (3) transformation of the kaolinite + substituted apatite to a kaolinite + crandallite mineral association. This paragenesis observed in lateritic soils is exactly the one observed in the Arago cave, except for the fact that in the third step two Al phosphates of different solubility, namely crandallite and montgomeryite, are observed here and co-exist in a metastable equilibrium. This coexistence has also been observed in the el-Tabun Palaeolithic cave located in the Middle East (Goldberg and Nathan, 1975). The Gibb's free energy of formation, ΔG_f^0, of pure montgomeryite ($Ca_2Al_2(PO_4)_3(OH).7H_2O$) and pure crandallite ($CaAl_3(PO_4)_2(OH)_5.H_2O$) is -7347.1 kJ/mol and −5594.1 kJ/mol, respectively (Nriagu, 1976; Vieillard, 1978). The metastability is, however, difficult to quantify due to the effect of impurities (such as Mg in montgomeryite (Moore and Araki, 1974) or Sr, Ba and rare earth elements in crandallite (Schwab *et al.*, 1989)) on the stability of these two minerals. Eventually, all montgomeryite will turn into crandallite and the crandallite + kaolinite mixture will itself turn to wavellite + kaolinite and ultimately to gibbsite (Vieillard *et*

al., 1979). Aluminium ions, released by clay minerals may also inhibit the dissolution of hydroxylapatite (Christoffersen and Christoffersen, 1985) and this may explain why the few bones well preserved within the decarbonated pocket are so rich in Al (corresponding profiles in Fig. 3*a*). Similarly, two types of hydroxylapatite of different crystallinities and thus probably different solubilities co-exist. The apatite found in preserved bones has a very high crystallinity index (Fig. 6 and Table 2), and thus may be assumed to be the stable thermodynamic phase, similar to 'apatite I' found at the bottom of the decarbonated pocket. In contrast, 'apatite II', present as amorphous coatings covering secondary minerals, has been formed more recently and probably represents a metastable phase.

In conclusion, the observation of well-preserved bones by PIXE, PIGME and XRD has confirmed previous diagenesis theories. In particular this structural and chemical study has identified: (1) the very high crystallinity of apatite which completely replaced carbonate hydroxylapatite; and (2) the presence in bones of Al, F, Fe and Zn which may be present either as ions adsorbed on apatite which act as dissolution inhibitors, or as ions precipitated in distinct mineral phases. Phyllosilicates were shown not to be stable in the original calcareous environment and to be transformed into montgomeryite and crandallite.

Acknowledgements

We gratefully acknowledge the constant support from the AGLAE team, particularly from Joseph Salomon and Thomas Calligaro, for running the accelerator. We also thank Anne-Marie Moigne for sampling and classifying bone artefacts from the Arago cave, and Jean-Claude Miskovsky, director of the CNRS-UMR 5590, for initiating this work. Both work at the Centre de Recherche Préhistorique in Tautavel. The samples from Les Peyrugues were provided by Michel Allard (SRA, Toulouse) and those from La Chrétienne M by Jean-Pierre and Anne Joncheray (FFESSM, Fréjus). We would also like to acknowledge the experimental work carried out by Vincent Ripoche, F content measurements on the fluorapatite standard by the CRPG in Nancy and critical comments on the manuscript by Jean-Claude Dran. This work was supported by a grant from the Swiss National Science Foundation to L.Q. and in part by a grant from the CNRS to L.C. (via FAUST-Grenoble).

References

Badone, E. and Farquhar, R.M. (1982) Application of neutron activation analysis to the study of element concentration and exchange in fossil bones. *J. Radioanalytical Chem.*, **69**, 291–311.

Beiner, M. (1983) Etude des minéraux lourds de la Caune de l'Arago et de son environnement. *Bull. de l'Assoc. fr. Quatern.*, **1**, 19–23.

Bocherens, H., Fizet, M., Mariotti, A., Gangloff, R.A. and Burns, J.A. (1994) Contribution of isotopic biogeochemistry (^{13}C, ^{15}N, ^{18}O) to the paleoecology of mammoths (*Mammuthus Primigenius*). *Hist. Biol.*, **7**, 187–202.

Boscher-Barré, N., Trocellier, P., Deschamps, N., Dardenne, C., Blondiaux, J. and Buchet, L. (1992) Nuclear microprobe study of trace element in archaeological bones. *J. Trace Microprobe Techn.*, **10**, 77–90.

Calligaro, T., MacArthur, J.D. and Salomon, J. (1996) An improved experimental setup for the simultaneous PIXE analysis of heavy and light elements with a 3 MeV proton external beam. *Nucl. Instr. Methods Phys. Res. B*, **109/110**, 125–8.

Christoffersen, M.R. and Christoffersen, J. (1985) The effect of aluminum on the rate of dissolution of calcium hydroxyapatite – a contribution to the understanding of aluminum-induced bone diseases. *Calc. Tiss. Int.*, **37**, 673–6.

Coote, G.E. and Vickridge, I. (1988) Application of a nuclear microprobe to the study of calcified tissues. *Nucl. Instr. Methods Phys. Res. B*, **30**, 393–397.

Elliott, T.A. and Grime, G.W. (1993) Examining the diagenetic alteration of human bone material from a range of archaeological burial sites using nuclear microscopy. *Nucl. Instr. Methods Phys. Res. B*, **77**, 537–47.

Goldberg, P.S. and Nathan, Y. (1975) The phosphate mineralogy of el–Tabun cave, Mount Carmel, Israel. *Mineral. Mag.*, **40**, 253–8.

Henderson, P., Marlow, C.A., Molleson, T.I. and Williams, C.T. (1983) Patterns of chemical change during bone fossilization. *Nature*, **306**, 358–60.

Iacumin, P., Cominotto, D. and Longinelli, A. (1996) A stable isotope study of mammal skeletal remains of mid-Pleistocene age, Arago Cave, Eastern Pyrenees, France. Evidence of taphonomic and diagenetic effects. *Palaeogeog., Palaeoclimatol., Palaeoecol.*, **126**, 151–60.

Kyle, J.H. (1986) Effect of post-burial contamination on the concentrations of major and minor elements in human bones and teeth – the implications for

palaeodietary research. *J. Archaeol. Sci.*, **13**, 403–16.

Lambert, J.B., Simpson, S.V., Szpunar, C.B. and Buikstra, J.E. (1985) Bone diagenesis and dietary analysis. *J. Human Evol.*, **14**, 477–82.

Lumley, H. de and Lumley, M.-A. de (1971) Découverte de restes humains anténéanderthaliens datés du Riss à la Caune de l'Arago (Tautavel, Pyrénées–Orientales). *C. R. Acad. Sci., Paris, D*, **272**, 1739–42.

Lumley, H. de, Fournier, A., Park, Y.C., Yokoyama, Y. and Demouy, A. (1984) Stratigraphie du remplissage Pléistocène moyen de la Caune de l'Arago à Tautavel. Etude de huit carottages effectués de 1981 à 1983. *L'Anthropologie (Paris)*, **88**, 5–18.

Maxwell, J.A., Campbell, J.L. and Teesdale, W.J. (1988) The Guelph PIXE software. A description of the code package. *Nucl. Instr. Methods Phys. Res. B*, **43**, 218–30.

Menu, M., Calligaro, T., Salomon, J., Amsel, G. and Moulin, J. (1990) The dedicated accelerator-based IBA facility AGLAE at the Louvre. *Nucl. Instr. Methods Phys. Res. B*, **45**, 610–4.

Michel, V., Ildefonse, Ph. and Morin, G. (1996) Assessment of archaeological bone and dentine preservation from Lazaret cave (Middle Pleistocene) in France. *Palaeogeog., Palaeoclimatol., Palaeoecol.*, **126**, 109–19.

Millard, A.R. and Hedges, R.E.M. (1995) The role of the environment in uranium uptake by buried bone. *J. Archaeol. Sci.*, **22**, 239–50.

Moore, P.B. and Araki, T. (1974) Montgomeryite, $Ca_4Mg(H_2O)_{12}[Al_4(OH)_4(PO_4)_6]$; its crystal structure and relation to vauxite, $Fe_2^{2+}(H_2O)_4[Al_4(OH)_4(H_2O)_4(PO_4)_4]4H_2O$). *Amer. Mineral.*, **59**, 843–50.

Mosser, C., Miskovsky, J.-C., Chevallier-Renaud, M.-C. and Larque, P. (1992) L'histoire et l'origine de sédiments préhistoriques décrites par les éléments traces des argiles. Exemple du remplissage de la Caune de l'Arago (Tautavel, Pyrénées-Orientales, France). *Mém. Soc. géol. Fr.*, **160**, 45–54.

Nriagu, J.O. (1976) Phosphate-clay mineral relations in soils and sediments. *Canad. J. Earth Sci.*, **13**(6), 719–36.

Parker, R.B. and Toots, H. (1980) Trace elements in bones as paleobiological indicators. In *Fossils in the Making,* (A.K. Behrensmeyer and A.P. Hill, eds). The University of Chicago Press, Chicago, pp. 197–207.

Pate, F.D. and Hutton, J.T. (1988) The use of soil chemistry data to address post-mortem diagenesis in bone mineral. *J. Archaeol. Sci.*, **15**, 729–39.

Perrenoud, C. (in press) La phosphatogenèse de la Caune de l'Arago (Tautavel, France): approche micromorphologique. In *Proc. 13th U.I.S.P.P. Congress, Forli* (1996).

Person, A., Bocherens, H., Saliège, J.-F., Paris, F., Zeitoun, V. and Gérard, M. (1995) Early diagenetic evolution of bone phosphate: an X-ray diffractometry analysis. *J. Archaeol. Sci.*, **22**, 211–21.

Pois, V. (1997) Apport de l'informatique à l'étude d'un gisement karstique. Exemple de la Caune de l'Arago à Tautavel (Pyrénées Orientales, France). *Quaternaire*, **8**, 143–7.

Price, T.D., Schoeninger, M.J. and Armelagos, G.J. (1985) Bone chemistry and past behaviour: an overview. *J. Human Evol.*, **14**, 419–47.

Price, T.D., Blitz, J., Burton, J. and Ezzo, J.A. (1992) Diagenesis in prehistoric bone: problems and solutions. *J. Archaeol. Sci.*, **19**, 513–29.

Runia, L.T. (1987) The chemical analysis of prehistoric bones; a paleodietary and ecoarcheological study of bronze age West-Friesland. *BAR International Series* **363**, 234 pp.

Schwab, R.G., Herold, H., Costa, M.L. da and Oliveira, N.P. de (1989) The formation of aluminous phosphates through lateritic weathering of rocks. In *Weathering; its products and deposits*, Vol. 2 (K.S. Balasubramaniam *et al.*, eds). Theophrastus Publications, Athens, pp. 369–86.

Simkiss, K. and Wilbur, K.M. (1989) *Biomineralization: cell biology and mineral deposition.* Academic Press Inc., San Diego. 337 pp.

Vieillard, P. (1978) *Géochimie des phosphates. Etude thermodynamique. Application à la genèse et à l'altération des apatites.* PhD thesis, Univ. Toulouse, Sciences géologiques, mémoire n° 51, Université Louis Pasteur, Strasbourg, 185 pp.

Vieillard, P., Tardy, Y. and Nahon, D. (1979) Stability fields of clays and aluminium phosphates: paragenesis in lateritic weathering of argillaceous phosphatic sediments. *Amer. Mineral.*, **64**, 626–34.

Williams, C.T. (1988) Alteration of chemical composition of fossil bones by soil processes and groundwater. In *Trace Elements in Environmental History,* (G. Grupe and B. Herrmann, eds). Springer Verlag, Berlin, 27–40.

[*Manuscript received 11 August 1997: revised 2 August 1998*]